Enhanced sensing of gas molecules by a 99.9% semiconducting carbon nanotube-based field-effect transistor sensor

Minsu Jeon, Bongsik Choi, Jinsu Yoon, Dong Myong Kim, Dae Hwan Kim, Inkyu Park, and Sung-Jin Choi

Citation: Appl. Phys. Lett. **111**, 022102 (2017); doi: 10.1063/1.4991970
View online: http://dx.doi.org/10.1063/1.4991970
View Table of Contents: http://aip.scitation.org/toc/apl/111/2
Published by the American Institute of Physics

Enhanced sensing of gas molecules by a 99.9% semiconducting carbon nanotube-based field-effect transistor sensor

Minsu Jeon,[1,a)] Bongsik Choi,[1,a)] Jinsu Yoon,[1] Dong Myong Kim,[1] Dae Hwan Kim,[1] Inkyu Park,[2,3,b)] and Sung-Jin Choi[1,b)]
[1]*School of Electrical Engineering, Kookmin University, Seoul 136-702, South Korea*
[2]*Department of Mechanical Engineering, KAIST, Daejeon 305-701, South Korea*
[3]*Mobile Sensor and IT Convergence Center, KAIST, Daejeon 305-701, South Korea*

(Received 16 March 2017; accepted 21 June 2017; published online 10 July 2017)

Carbon nanotubes (CNTs) have been regarded as a promising material for highly sensitive gas sensors due to their excellent material properties combined with their one-dimensional structural advantages, i.e., a high surface-to-volume ratio. Here we demonstrate a CNT-based gas sensor based on assembling highly purified, solution-processed 99.9% semiconducting CNT networks bridged by palladium source/drain electrodes in a field-effect transistor (FET) configuration with a local back-gate electrode. We investigated the gas responses of the CNT-FETs under different controlled operating regimes for the enhanced detection of H_2 and NO_2 gases using sensors with various physical dimensions. With the aid of the CNTs with high semiconducting purity (99.9%), we achieved excellent electrical properties and gas responses in the sensors and clearly determined that the operating regimes and physical dimensions of the sensors should be appropriately adjusted for enhanced sensing performance, depending on the gas molecules to be detected. *Published by AIP Publishing.* [http://dx.doi.org/10.1063/1.4991970]

As transparent, conductive, and flexible materials, carbon nanotubes (CNTs) have attracted considerable attention for applications in several areas because of their many outstanding properties, including excellent electrical, mechanical, chemical, optical, and thermal properties.[1–9] Specifically, these properties render them promising candidates in broad areas of electronic applications. For example, CNTs have been considered an ideal material for gas sensing due to their intrinsically high surface-to-volume ratio originating from their nanosized, one-dimensional structure.[5,10–14] Thus, the electrical properties of CNTs can be extremely sensitive to charge transfer and chemical doping effects by various molecules. For instance, adsorption of electron-withdrawing (e.g., NO_2, O_2)[10–14] or donating (e.g., NH_3)[11,16,17] molecules on CNTs can cause charge transfer between the CNTs and gas molecules. Notably, if semiconducting CNTs are employed for sensing, the charge transfer can lead to dramatic changes in their electrical conductance (or resistance), which serves as the basis for highly sensitive CNT-based gas sensors. In addition to sensing molecules adsorbed on CNTs, i.e., gas molecules that can react with the CNTs themselves by charge transfer, various other gas molecules can also be detected in a CNT-based gas sensor when gas-sensitive metal electrodes are in contact with the CNTs. For example, hydrogen (H_2) can be detected in a CNT-based gas sensor using a prominent and well-studied H_2-sensitive electrode, such as palladium (Pd).[6,18–21] If the Pd contacts the semiconducting CNTs, a Schottky barrier (SB) can be formed at the interface between the Pd electrode and semiconductor CNTs; hence, the Schottky barrier height (SBH) can be modulated, resulting from the change in the Pd work function caused by the adsorption of H_2 molecules.[6,18–23] This SBH modulation could be a useful sensing element for the detection of H_2 because the electric current over and through the SB arising from thermionic emission and tunneling is exponentially dependent on the change in the SBH. Furthermore, the "nanoscale" SB contact comprising the semiconducting CNTs and electrodes has its own advantage, as the open contact geometry allows unhindered diffusion of gas molecules to the barrier and leads to a beneficial effect on the response dynamics, compared to a "macroscopic" SB contact.[20]

To detect various gas molecules, as mentioned, on the basis of the CNT-based sensors, the central sensing unit could be a field-effect transistor (FET) structure where semiconducting CNTs and gas-sensitive metal electrodes are employed for the channel and source/drain (S/D) electrodes, respectively. Using the reactions of gas molecules with CNTs themselves and the gas-sensitive metal electrodes, a significant change in current flow can occur, resulting from the respective intermolecular charge transfer and SBH modulation. The detection of various gas molecules in CNT-based FET gas sensors has been reported,[6,11,13–16,19–21] but enhanced sensing methods for gas molecules having different sensing mechanisms, i.e., reacting with CNTs and/or gas-sensitive metal electrodes, have not yet been reported sufficiently. Controlling the operating regime, i.e., the operating bias conditions in CNT-based FET gas sensors, could be a good method to enhance the sensor operations, depending on the gas molecules to be detected. Moreover, the fundamental physical parameters of the CNT-based FET gas sensors affecting the sensing performances have not been established. Specifically, CNT-based FETs composed of a percolated network channel formed of CNTs with high semiconducting purity (i.e., above 99%) have been considered to be a platform for next-generation thin-film transistors

[a)]M. Jeon and B. Choi contributed equally to this work.
[b)]Electronic addresses: inkyu@kaist.ac.kr and sjchoiee@kookmin.ac.kr. Tel.: +82-2-910-5543. Fax: +82-2-910-4449.

(TFTs) and sensors, but there have been few studies on gas sensing using this device structure.

Here, we demonstrate an enhanced sensing method using two representative gas molecules, H_2 and NO_2, having different sensing mechanisms in the CNT-based FET gas sensor comprising highly purified, pre-separated 99.9% semiconducting CNT networks and Pd S/D electrodes. Fortunately, Pd has been demonstrated to have excellent material compatibility with CNTs, showing Ohmic contact;[24,25] hence, excellent electrical and sensor performances were simultaneously achieved.[6,19–21] Using the 99.9% semiconducting CNT-based FET gas sensor with Pd S/D electrodes, we investigated the enhanced sensing method via controlling the operating regimes and physical dimensions of the sensors. Importantly, with the aid of the highly purified, pre-separated 99.9% semiconducting CNT networks in the channel of the FET-based gas sensor, excellent electrical properties were attained with a high on/off current ratio. This leads to distinguishable operating regimes of the devices, such as subthreshold and linear (or saturation) regimes, which provides an excellent platform to investigate the sensor sensitivity by controlling the operating regimes. Furthermore, the sensor structure based on the 99.9% semiconducting CNT network channel results in excellent device yield, electrical properties, and uniformity, which is essential for practical applications. We believe that our work will be helpful in guiding and optimizing the design of highly sensitive CNT-based FET gas sensors.

A schematic of our CNT-based FET gas sensor for the detection of H_2 and NO_2 molecules having different sensing mechanisms is shown in Fig. 1(a). Highly purified, pre-separated 99.9% semiconducting CNTs were utilized for the formation of randomly networked CNT channels. For the effective modulation of the operating regimes of the CNT-based FET gas sensor, we employed a local back-gate structure. Our CNT-based FET gas sensor was fabricated by the following processes: First, a highly p-doped silicon wafer with a thermally grown 50-nm-thick SiO_2 layer was used as a starting substrate. To form the local back-gate, a 30-nm-thick Pd layer was deposited and patterned using thermal evaporation and a lift-off process. Then, a 40-nm-thick Al_2O_3 layer was deposited by atomic layer deposition (ALD) as a gate dielectric, followed by the deposition of

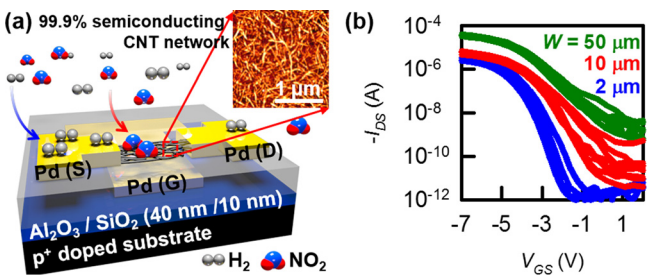

FIG. 1. (a) Device schematic of the CNT-based gas sensor based on highly purified, pre-separated 99.9% semiconducting CNTs bridged by Pd S/D electrodes in a FET configuration with a local back-gate. AFM image (z-scale is 10 nm) of the randomly networked CNT channel used in this work. (b) The transfer characteristics of CNT-based FET gas sensors with various W values ($W = 2$ μm, 10 μm, and 50 μm) and various L values from 1.9 μm to 3.0 μm.

10-nm-thick SiO_2 layer by plasma-enhanced chemical vapor deposition (PECVD) on which the amine-terminated surface was sequentially formed from a poly-L-lysine solution (0.1% w/v in water; Sigma Aldrich). After the formation of the surface, randomly networked, highly purified, pre-separated 99.9% semiconducting CNT channels were created. Afterward, to form S/D electrodes, 2-nm-thick titanium (Ti) and 30-nm-thick Pd layers were sequentially deposited and patterned by thermal evaporation and a lift-off process. Finally, because the CNTs covered the entire wafer, an additional photolithography step combined with O_2 plasma was used to remove the unwanted CNTs outside the channel region. In this step, the width (W) and length (L) of the CNT network channel were defined clearly. The W values of the devices ranged from 2 μm to 50 μm to evaluate the effect of the physical dimension of the sensors on the sensor responses; the L values of the devices were fixed at 2.8 μm. The atomic force microscopy (AFM) images of the CNT network channel is also shown in Fig. 1(a). The AFM image reveals that the semiconducting CNTs are uniformly percolated on the SiO_2 surface. The average CNT densities obtained from the working device were found to be approximately 78 ± 3 tubes/μm^2.

First, we compared the transfer curves of the CNT-based FET gas sensor with different W values (2 μm, 10 μm, and 50 μm) and with different L values ranging from 1.9 μm to 3.0 μm, as shown in Fig. 1(b). Note that as the W value increased, the average on/off current ratio was reduced from 10^6 to 10^4, even though we used CNTs with above 99% semiconducting purity (i.e., 99.9%) in the network channel. Given that 0.1% of CNTs are still metallic, the most straightforward explanation for this observation is that the probability of a metallic interconnection between the S/D electrodes still existed and increased with an increase in W value of the devices; hence, further purification above 99.9% semiconducting might be required. Nevertheless, excellent electrical properties were achieved from a total of 20 CNT-based FETs, such as the maximum mobility (μ) of 91.25 $cm^2 V^{-1} s^{-1}$ and transconductance (g_m) of 1.47 μS with the aid of the high-density network produced from the CNTs with high semiconducting purity (99.9%).[26,27] Moreover, we observed that the CNT-based FET gas sensor normally exhibits an initial p-type behavior in an ambient environment due to the adsorption of oxygen molecules and moisture and the large work function of the Pd in S/D electrodes.[24,25]

Next, using the CNT-based FET gas sensor with Pd S/D electrodes, we performed gas sensing experiments to detect the two representative gas molecules, i.e., H_2 and NO_2, as shown in Figs. 2(a) and 2(b), respectively. The CNT-based FET gas sensor was examined in the vacuum chamber equipped with the probe station. The H_2 was injected into the gas inlet by mixing dry synthetic air (79% N_2 and 21% O_2) and 0.1% H_2 in the air. Additionally, the NO_2 was injected into the gas inlet using pure N_2 and 0.01% NO_2 mixed in the N_2. The H_2 and NO_2 gas flow rates were maintained at 100 standard-cubic-centimeters per minute (sccm) and 1000 sccm, respectively. The gas concentrations of H_2 and NO_2 were controlled by the flow rate of each gas using mass flow controllers (MFCs). The electrical performances of the CNT-based FET gas sensors during the exposure of

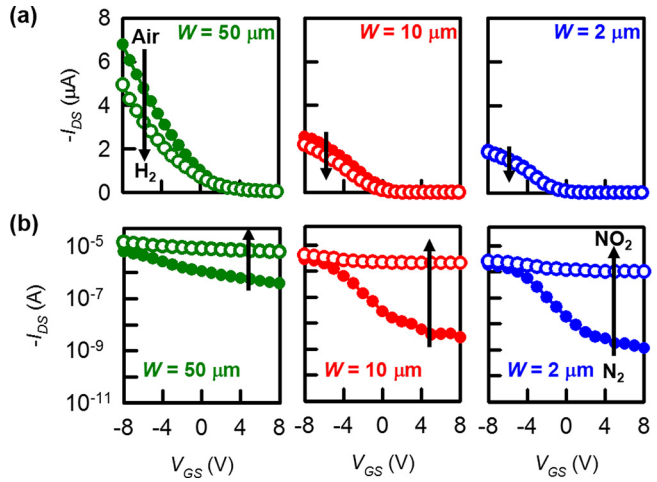

FIG. 2. The transfer characteristics for CNT-based FET gas sensors with W values of 2 μm, 10 μm, and 50 μm before and after exposure to (a) H_2 at room temperature and (b) NO_2 at 150 °C at a V_{DS} of −0.5 V. For improved recovery and fast response, the NO_2 responses were measured at the higher temperature.

H_2 and NO_2 were measured using Keithley 4200. Note that H_2 responses were measured at 25 °C, but NO_2 responses were measured at the higher temperature of 150 °C for enhanced recovery and a fast response time. Moreover, at a higher temperature, the charge transfer between CNTs and NO_2 molecules can be dominant over the SB modulation by NO_2 adsorption.[15,16] Therefore, a clear difference between the sensing mechanisms of H_2 and NO_2 gas molecules can be achieved.

First, for the measurement of gas responses, the transfer curves of the CNT-based FET gas sensors with different W values (2 μm, 10 μm, and 50 μm) and a fixed $L = 2.8$ μm were measured at a drain-to-source voltage (V_{DS}) of –0.5 V in ambient conditions, and subsequently, the transfer curves were repeatedly measured after exposure to 0.1% H_2 for 180 s, as shown in Fig. 2(a). Exposing the H_2 molecules on the CNT-based FET gas sensor to the Pd S/D electrodes in the chamber, the H_2 molecules reacted with the Pd S/D electrodes and were separated into hydrogen atoms. The separated hydrogen atoms were believed to be dissolved into the Pd electrode, resulting in the formation of Pd hydride (PdH_x). This would quickly lower the electronic work function of Pd and create a prominent SB at the interface between the Pd electrodes and semiconducting CNTs,[6,18–21] resulting in the reduced injection of major carriers in the CNT-based FETs, i.e., hole carriers into the CNTs. As a result, a decrease in I_{DS} after H_2 exposure was observed in the transfer curves because the formation of the SB at the interface upon H_2 exposure can increase the corresponding contact resistance (R_c).[28] Note that the H_2 responses in the devices became noticeable with an increase in W values of the CNT-based FET sensors, which is closely related to the sensing mechanisms for H_2 molecules (as will be discussed later in detail). Moreover, we performed the same experiment for the NO_2 response, as shown in Fig. 2(b), where 0.006% NO_2 was injected for 150 s. Oxidizing gases such as NO_2 adsorb on the CNT surfaces and can likely extract electrons from semiconducting CNTs,[11–14] thereby leading to an expansion of the conducting channel, i.e., decreased CNT resistance. As a result, an overall significant increase in I_{DS} was observed in the transfer curves. In the transfer curves, the gating effect in the transistor operation seemed to disappeared, observed from such a significant increased I_{DS}. However, this is mostly attributed to high concentration of NO_2 that we used; hence, it is expected that the gating effect can be restored if we employ lower concentration of NO_2. Note also that unlike the H_2 responses, more significant NO_2 responses were obtained for narrower W devices, which is related to the sensing mechanism of NO_2 gas molecules (as will also be discussed later in detail).

To further investigate and enhance the gas responses in the CNT-based FET gas sensors, we measured the transient responses under H_2 exposure for various V_{GS} values to control the operating regimes of the devices. The responses were measured on the devices with different W dimensions, as shown in Fig. 3(a). The CNT-based FET gas sensors were sequentially tested with gas concentrations of H_2 from 0.02% to 0.1% with alternating 180 s periods of H_2 exposure and 300 s periods of dried air. We observed that the I_{DS} clearly decreased with the injection of H_2, and this change became greater with higher concentrations of H_2. However, the I_{DS} increased again, i.e., recovered, with the injection of dried air, which indicates that the CNT-based FET gas sensor is fully reversible for H_2 detection. The overall transient H_2 responses indicate that for the device with a narrow W value of 2 μm, the I_{DS} does not noticeably decrease upon H_2 exposure; only minimal responses can be shown for the narrow W device, even at a more negative V_{GS} regime. In contrast, the devices with relatively larger W value, such as 50 μm, showed appreciable decreases in I_{DS} upon H_2 exposure, which was consistent with the results anticipated from the transfer properties shown in Fig. 2(a). Importantly, it was clearly observed that the applied V_{GS} during the sensor measurements affected the H_2 responses. Note that the decrease in

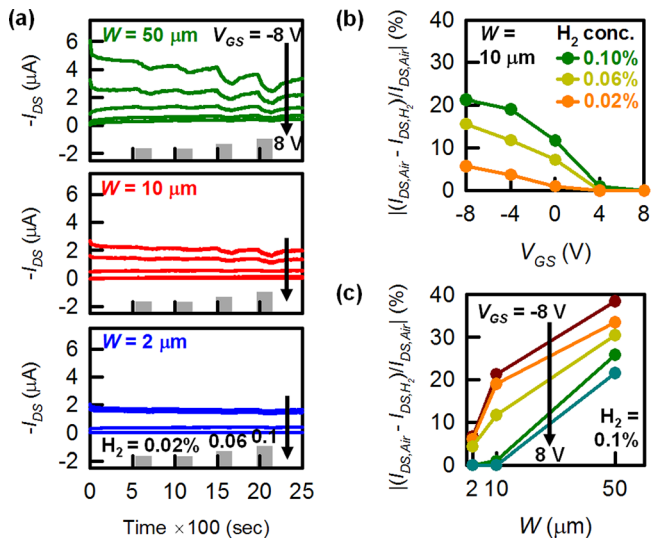

FIG. 3. (a) Real-time detection of H_2 molecules with various concentrations on the CNT-based FET sensors with W values of 2 μm, 10 μm, and 50 μm at room temperature at different V_{GS} values. Summarized results of percentage relative responses of I_{DS} for (b) different V_{GS} values and (c) physical dimensions. The voltages were applied to the local back-gate to adjust the operating regime of the CNT-based FET sensors from linear (−8 V) to subthreshold (or depletion) regimes (8 V).

I_{DS} became significant as V_{GS} decreased from 8 V to −8 V, regardless of different W values. To obtain a more comprehensive understanding of H_2 responses, we summarized the results of H_2 responses for various concentrations of H_2 with various V_{GS} values and physical dimensions of the sensor using the percentage relative responses, defined as $|(I_{DS,Air} - I_{DS,H2})/I_{DS,Air}| \times 100$, as shown in Figs. 3(b) and 3(c). The results showed that the sensor responses increased in the devices with larger W value at more negative V_{GS} values.

The decrease in I_{DS} upon exposure to H_2 gas is mainly attributed to the increased R_c caused by the decreased work function of Pd from the adsorption of H_2. However, in CNT-based FET sensors, especially for CNT network-based FET sensors, the change in R_c by H_2 adsorption is generally small,[29] such that the change in current flow, i.e., I_{DS}, is not appreciable because the portion of R_c in the total resistance (R_T) of the CNT-based FET sensor is too small compared to the channel resistance (R_{ch}). Generally, in a CNT "network"-based FET structure, the value of R_{ch} is relatively large, caused by large numbers of CNT-CNT junctions.[30] Therefore, to effectively detect H_2 responses in a CNT-based FET sensor, the portions of R_c and R_{ch} in R_T should be high and low, respectively. Such conditions can be created by adjusting the operating regimes. That is, a more negative V_{GS} value to adjust the operating regime to a linear operating regime renders the CNT network channel highly "conductive," i.e., transparent; hence, the portion of R_c in R_T becomes larger, and H_2 detection is correspondingly more favorable at such a condition. In addition, the portion of R_c in R_T can be enhanced by simply increasing the W value of the devices, resulting from the decrease in R_{ch} such that the noticeable detection of H_2 would be possible.

Next, we also investigated the transient responses to NO_2 exposure at various concentrations at various V_{GS} values in CNT-based FET sensors with different W values, as shown in Fig. 4(a). The CNT-based FET gas sensor sequentially detected gas concentrations of NO_2 from 0.002% to 0.006% with alternating 150 s periods of NO_2 exposure and 2500 s periods of N_2 exposure. Again, note that we performed the NO_2 experiment responses at the higher temperature of 150 °C (compared to the H_2 responses at room temperature) because of the enhanced recovery and fast response. It was observed that the I_{DS} clearly increased upon the injection of NO_2, and it exhibited greater changes with the increasing concentrations of NO_2. Moreover, the I_{DS} decreased (i.e., recovered) to the baseline level upon the injection of N_2. However, for some of the sensors, the I_{DS} values were not fully recovered to the baseline level, which was most likely due to large hysteresis in the CNT-based FET sensors; hence, it should be improved for practical application. It is worthwhile to note that the behaviors of the NO_2 responses are entirely different from the H_2 responses: Higher responses were observed for NO_2 with the device with a narrower W value and at a more positive V_{GS} value, i.e., 8 V, as expected in Fig. 2(b). The transient responses for cyclic NO_2 exposure are summarized using $|(I_{DS,N2} - I_{DS,NO2})/I_{DS,N2}| \times 100$ in Figs. 4(b) and 4(c).

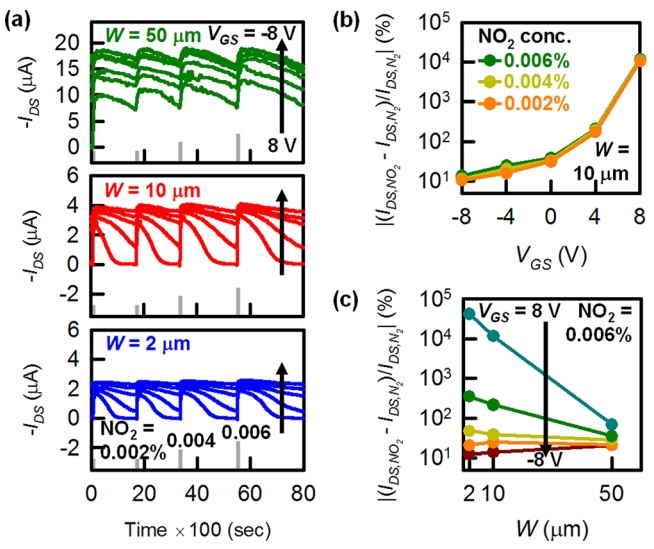

FIG. 4. (a) Real-time detection of NO_2 molecules with various concentrations on the CNT-based FET sensors with W values of 2 μm, 10 μm, and 50 μm at 150 °C at different V_{GS} values. Summarized results of percentage relative responses of I_{DS} for (b) different V_{GS} values and (c) physical dimensions. The voltages were applied to the local back-gate to adjust the operating regime of the CNT-based FET sensors from linear (−8 V) to subthreshold (or depletion) regimes (8 V).

From the adsorbed NO_2 molecules on the CNT surfaces, the electrons in the valence band of the semiconducting CNTs were extracted via the following reaction, i.e., charge transfer: $NO_2 + e^- \rightarrow NO_2^-$.[11–14] This extraction leads, in turn, to an expansion of the hole accumulation layer, i.e., a decrease in the resistance of the semiconducting CNTs, which means that a high sensitivity can be obtained in the subthreshold regime (also called depletion regimes) at the V_{GS} values shifting to the positive direction, where the gating effect of the gas molecules bound on the channel surface of FET-based sensors is most effective due to the reduced screening of carriers in the channel. This is in sharp contrast to the H_2 responses. Moreover, a sharp distinction from the H_2 responses can be found in the measurement results of the devices with various W values. For NO_2 detection, the responses became prominent with decreasing W values, but for H_2 detection, higher responses were obtained with increasing W values. This is closely related to the electrical performance of the CNT-based FET sensors: the higher on/off current ratio was attained in the device with the narrower W value. For larger W devices, there are still many metallic CNTs in the percolated network channel, even though we employed CNTs with the high semiconducting purity of 99.9%. Therefore, the resistance of these metallic CNTs could hardly be controlled by charge transfer, such that lower responses were observed in the devices with larger W values. Therefore, simultaneous detection of H_2 and NO_2 could be accomplished based on CNT-based FET sensors with large W values but with a high on/off current ratio. Such devices can be made using CNTs with above 99.9% semiconducting purity; hence, multiple gas molecules having different sensing mechanisms might be detected in a single CNT-based FET sensor, and their sensitivity could be improved by adjusting the V_{GS} values to control the operating regimes. Note that although we did not measure gas response measurements of NO_2 diluted in dry air for practical application or any molecules in a humid environment, our results pave the way toward the optimization of sensing performances and sensor design.

In conclusion, we demonstrated enhanced sensing responses to representative gas molecules, H_2 and NO_2, having different sensing mechanisms using a highly purified, pre-separated 99.9% semiconducting CNT network FET sensor. With the aid of the excellent electrical properties of the 99.9% semiconducting CNT-based FET sensor, we clearly showed that, according to the sensing gas molecules being sensitive to either the CNTs themselves or the S/D metal electrodes, the sensor design and operating regimes could be chosen carefully. Although we only demonstrated sensing experiments using two representative gas species, we believe that our studies can be expanded to other gas responses, providing an essential guideline to realize multiple detections for practical electronic nose applications.

This work was supported by the National Research Foundation (NRF) of Korea under Grant Nos. 2016R1A2B4011366 and 2016R1A5A1012966, and partially funded by the Future Semiconductor Device Technology Development Program (Grant No. 10067739) by MOTIE (Ministry of Trade, Industry and Energy) and KSRC (Korea Semiconductor Research Consortium).

[1]Q. Cao, H.-S. Kim, N. Pimparkar, J. P. Kulkarni, C. Wang, M. Shim, K. Roy, M. A. Alam, and J. A. Rogers, Nature **454**, 495 (2008).
[2]J. Zhang, C. Wang, and C. Zhou, ACS Nano **6**, 7412 (2012).
[3]E. Artukovic, M. Kaempgen, D. S. Hecht, S. Roth, and G. Gruner, Nano Lett. **5**, 757 (2005).
[4]C. Wang, J. Zhang, K. Ryu, A. Badmaev, L. G. D. Arco, and C. Zhou, Nano Lett. **9**, 4285 (2009).
[5]Q. Cao and J. A. Rogers, Adv. Mater. **21**, 29 (2009).
[6]A. Javey, J. Guo, Q. Wang, M. Lundstrom, and H. Dai, Nature **424**, 654 (2003).
[7]M. Amjadi, Y. J. Yoon, and I. Park, Nanotechnology **26**, 375501 (2015).
[8]D. Kwon, T.-I. Lee, J. Shim, S. Ryu, M. S. Kim, S. Kim, T.-S. Kim, and I. Park, ACS Appl. Mater. Interfaces **8**, 16922 (2016).
[9]H. Lee, D. Kwon, H. Cho, I. Park, and J. Kim, Sci. Rep. **7**, 39837 (2017).
[10]P. G. Collins, K. Bradley, M. Ishigami, and A. Zettl, Science **287**, 1801 (2000).
[11]J. Kong, N. R. Franklin, C. Zhou, M. G. Chapline, S. Peng, K. Cho, and H. Dai, Science **287**, 622 (2000).
[12]J. Li, Y. Lu, Q. Ye, M. Cinke, J. Han, and M. Meyyappan, Nano Lett. **3**, 929 (2003).
[13]P. Qi, O. Vermesh, M. Grecu, A. Javey, Q. Wang, and H. Dai, Nano Lett. **3**, 347 (2003).
[14]H. Li, C. Wen, Y. Zhang, D. Wu, S.-L. Zhang, and Z.-J. Qiu, Sci. Rep. **6**, 21313 (2016).
[15]J. Zhang, A. Boyd, A. Tselev, M. Paranjape, and P. Barbara, Appl. Phys. Lett. **88**, 123112 (2006).
[16]N. Peng, Q. Zhang, C. L. Chow, O. K. Tan, and N. Marzari, Nano Lett. **9**, 1626 (2009).
[17]Z.-D. Lin, S.-J. Young, and S.-J. Chang, IEEE Trans. Electron Devices **63**, 476 (2016).
[18]Y. M. Wong, W. P. Kang, J. L. Davidson, A. Wisitsora-At, and K. L. Soh, Sens. Actuators, B **93**, 327 (2003).
[19]M. Zhang, L. L. Brooks, N. Chartuprayoon, W. Bosze, Y.-H. Choa, and N. V. Myung, ACS Appl. Mater. Interfaces **6**, 319 (2014).
[20]M. Ganzhorn, A. Vijayaraghavan, S. Dehn, F. Hennrich, A. A. Green, M. Fichtner, A. Voigt, M. Rapp, H. Lohneysen, M. C. Hersam, M. M. Kappes, and R. Krupke, ACS Nano **5**, 1670 (2011).
[21]B. Choi, D. Lee, J.-H. Ahn, J. Yoon, J. Lee, M. Jeon, D. M. Kim, D. H. Kim, I. Park, Y.-K. Choi, and S.-J. Choi, Appl. Phys. Lett. **107**, 193108 (2015).
[22]Y. Sun and H. H. Wang, Adv. Mater. **19**, 2818 (2007).
[23]J. Kong, M. G. Chapline, and H. Dai, Adv. Mater. **13**, 1384 (2001).
[24]Z. Chen, J. Appenzeller, J. Knoch, Y.-M. Lin, and P. Avouris, Nano Lett. **5**, 1497 (2005).
[25]Y. Nosho, Y. Ohno, S. Kishimoto, and T. Mizutani, Nanotechnology **17**, 3412 (2006).
[26]D. Lee, M.-L. Seol, D.-I. Moon, P. Bennett, N. Yoder, J. Humes, J. Bokor, Y.-K. Choi, and S.-J. Choi, Appl. Phys. Lett. **104**, 143508 (2014).
[27]N. Rouhi, D. Jain, K. Zand, and P. J. Burke, Adv. Mater. **23**, 94 (2011).
[28]S. M. Sze and K. K. Ng, *Physics of Semiconductor Devices* (John Wiley & Sons, Inc., 2007), pp. 187–191.
[29]J. Sippel-oakley, H.-T. Wang, B. S. Kang, Z. Wu, F. Ren, A. G. Rinzler, and S. J. pearton, Nanotechnology **16**, 2218 (2005).
[30]J.-W. Do, D. Estrada, X. Xie, N. N. Chang, J. Mallek, G. S. Girolami, J. A. Rogers, E. Pop, and J. W. Lyding, Nano Lett. **13**, 5844 (2013).